

Microstructure of otoliths in larval and juvenile Shishamo smelt *Spirinchus lanceolatus*, a cold-water fish species

Takehiro Yoshida¹, Mitsuhiro Nakaya^{2*}, Yoshifumi Konno³, Hisaya Nii³, Junki Ataka⁴, Ryuya Hasegawa⁴,
Nozomi Okada^{4,5}, Tetsuya Takatsu²

¹Graduate School of Fisheries Sciences, Hokkaido University, 3-1-1, Minato, Hakodate, Hokkaido 041-8611, Japan. ²Faculty of Fisheries Sciences, Hokkaido University, 3-1-1, Minato, Hakodate, Hokkaido 041-8611, Japan. ³Hokkaido Aquaculture Promotion Corporation, Sapporo, Hokkaido 060-0003, Japan. ⁴Mariculture Fisheries Research Institute, Hokkaido Research Organization, Muroran, Hokkaido 051-0013, Japan. ⁵Present address: Central Fisheries Research Institute, Hokkaido Research Organization, Yoichi, Hokkaido 046-8555, Japan.

*Corresponding author, email: mnakaya@fish.hokudai.ac.jp

Abstract

We examined the daily periodicity of otolith increment formation in reared Shishamo smelt *Spirinchus lanceolatus* larvae, and investigated the growth history of wild-caught larvae. The mean body length of newly hatched larvae was 8.4 mm, and the mean otolith radius was 12.7 μm (sagitta) and 12.4 μm (lapillus), respectively. Both otoliths displayed a check mark at hatching (1st check), and an additional check mark was observed later (2nd check). The relationship between the number of increments formed outside the 1st check on both otoliths (I_s , I_l) and age (A_c , days) was described by regression lines ($I_s = 0.86A_c$ ($n = 38$, $r^2 = 0.992$, $p < 0.01$), $I_l = 0.49A_c$ ($n = 24$, $r^2 = 0.932$, $p < 0.01$)), where the slopes significantly differed from 1 (t-test, both $p < 0.01$). We also examined the relationship between the number of increments outside the 2nd check (I'_s , I'_l) and age (A_c , days) for both otoliths. As a result, the regression lines ($I'_s = 0.99A_c - 19.5$ ($n = 26$, $r^2 = 0.996$, $p < 0.01$), $I'_l = 0.61A_c - 16.3$ ($n = 15$, $r^2 = 0.928$, $p < 0.01$)) showed that the slope for the sagitta was not significantly different from 1 (t-test, $p = 0.38$), while the lapillus was significantly different from 1 (t-test, $p < 0.01$). These results suggest that daily countable increments only form after the 2nd check mark in the sagitta. One possible reason why daily periodicity was not confirmed between the 1st and 2nd checks on both otoliths is that the increment width during this period was so narrow that it could not be distinguished under an optical microscope. This phenomenon has also been reported in cold-water fish species such as Atlantic herring and European sardine. Therefore, for cold-water fish species, which have increments after hatching that are generally difficult to distinguish, it is reasonable in age estimation to count increments only after they are clearly visible, and to compensate for earlier periods using check mark positions and growth indices. Based on the results of the rearing experiments, we examined the number and width of otolith increments in Shishamo smelt larvae and juveniles collected by sledge net along the Mukawa and Sarugawa coasts during June–July in 2023 and 2024. The ranges of hatching dates in both 2023 and 2024, calculated from age and sampling date, were respectively March 29–April 27 and March 23–April 27. A significant allometric relationship ($r^2 = 0.959$, $p < 0.001$) was found between otolith radius (OR, μm) and body length (BL, mm). The mean back-calculated body lengths of wild-caught individuals in 2023 and 2024 estimated using the Biological Intercept Method were respectively 11.4 mm and 11.3 mm at 20 days old, 17.0 mm and 17.6 mm at 40 days old, 21.8 mm and 23.3 mm at 60 days old, and 27.6 mm and 31.2 mm at 80 days old.

Key words: early life stages; otolith daily increment; Shishamo smelt; *Spirinchus lanceolatus*; validation

Introduction

Fluctuations in marine fishery resources are largely attributed to the survival rate during the early life stages (Hjort 1914). Since otolith daily increment analysis can be used to clarify the hatching date and growth history of individual larvae and juveniles (Campana and Neilson 1985), use of this method has

enabled significant contributions to studies on the early life history, which strongly affects recruitment in marine fish populations (Laroche et al. 1971; Jenkins 1987; Maillet and Checkley Jr 1991; Noichi et al. 1994; Bailey et al. 1995). Especially in species inhabiting relatively warm waters, such as Japanese sardine *Sardinops melanostictus* and Japanese jack

mackerel *Trachurus japonicus*, distinct increments are observed on otoliths immediately after hatching (Hayashi et al. 1989; Xie et al. 2005), and the use of these analyses have been widely adopted (Takahashi et al. 2008; Xie and Watanabe 2005).

On the other hand, in species such as Atlantic herring *Clupea harengus* and European sardine *Sardina pilchardus*, which spend their larval and juvenile phases in relatively cold waters, clarification of daily increments has been found to be difficult for some time after hatching due to the narrow width of otolith increments under low water temperatures (Campana et al. 1987; Soares et al. 2021). The primary cause is thought to be that when increment width falls below approximately 0.3 μm , the resolution limit of optical microscopes makes it difficult to count the increments (Campana et al. 1987).

Shishamo smelt *Spirinchus lanceolatus* is a species of cold-water fish found only along the Pacific coast of Hokkaido (Mori 2003). The catch of this species in the southern Hokkaido Pacific area exceeded 1,000 tons in the 1960s, but from 1995 to 2011 has mostly stayed in the range of 100–250 tons. There was a sharp decline to 12–36 tons from 2012 to 2015, followed by a slight recovery, but the catch fell below 1 ton in 2022, and fishing has been suspended as a resource recovery measure since 2023 (Saibai suisan shikenjyou 2025).

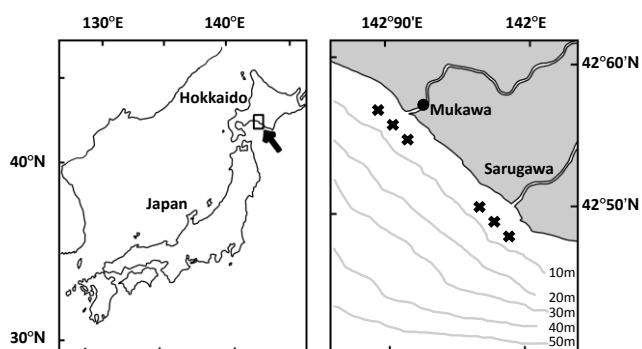


Fig. 1. Location of study area (left). The solid circle indicates the location where a survey was conducted to collect mature fish, and the areas marked with crosses represent regions where a sledge net was towed for wild larval fish sampling (right). Lines in sea area show the isobaths.

Regarding the ecology during the early life history, field studies have revealed suitable river conditions for spawning and migratory spawning behavior (Nii et al. 2006; Ishida 2020). Specifically, adults migrate upstream around November to spawn on riverbeds, with the eggs hatching in April or May of the following year and the larvae being immediately transported to the sea (Mori 2003). In coastal areas, they transition from a pelagic to a demersal lifestyle from mid- to late May (Torao and Kudo 2013). Although knowledge regarding seed production under hatchery conditions has been documented (Ishida 2016; Hokkaido Aquaculture Promotion Corporation 2017), details about growth during the larval stage in the wild have not been clarified. Furthermore, insights into otolith daily increment analysis—an effective method for such studies—including the daily periodicity of increment formation and otolith ultrastructure, remain unknown.

In this study, (1) we examine the daily periodicity of microincrement formation in Shishamo smelt larvae obtained from rearing experiments, particularly elucidating the characteristics of otolith increment formation in cold-water fish, which are considered to have slow early growth. Further, based on these findings, (2) we estimate the hatching season and growth process of larvae and juveniles collected from the southern Hokkaido Pacific area.

Materials and Methods

Validation of Daily Increment Formation

Rearing of Shishamo Smelt Larvae

On November 11, 2022, broodstock (70 females and 72 males, total length range: females 99.2–152.0 mm, males 121.7–157.5 mm) were collected using a fukube net (a type of set net) in the Mukawa River, Hokkaido, by Iburi district Shishamo fisheries promotion council (Fig. 1). Eggs and sperm were obtained and fertilized artificially using the dry method to produce fertilized eggs. The fertilized eggs were placed in 30-liter round tanks and maintained in a constant temperature room

at 3.4 ± 2.65 °C (mean \pm SD), with the temperature regime adjusted based on accumulated thermal units (Omi 1977). Approximately 5,000 hatched larvae were transferred to a 500 L round tank and reared at a mean water temperature of 13.9 ± 4.43 °C (mean \pm SD) over the entire rearing period, based on the natural seawater temperatures experienced by migrating larvae in the coastal areas of the Mukawa and Sarugawa rivers, which were represented by the water temperatures observed from April to May at the Tomihama Fishing Port near the mouth of the Sarugawa river. Larval rearing was conducted under a photoperiod of approximately 15 hours per day (7:00–22:00 lights on), matching the natural photoperiod from spring to early summer in the Mukawa region. Feeding started on the second day post-hatch. From 2 to 8 days after hatching (DAH), newly hatched Vietnamese *Artemia Artemia* sp. was provided; from 8 to 22 DAH, *Artemia* sp. enriched with Marine Gross EX (Marintech Co., Ltd., Aichi), a DHA-rich microalgae supplement, was used; from 22 DAH onward, a combination of formulated feed (Wakauo, Nosan Corporation, Kanagawa) and enriched *Artemia* from the Great Salt Lake (*Artemia franciscana*) was provided. It has also been reported that the survival rate of larval Shishamo smelt increases when *Nannochloropsis* or freshwater *Chlorella* is added to the rearing water (Hokkaido Aquaculture Promotion Corporation 2017). Therefore, refrigerated *Nannochloropsis* (Yanmarine K-1, Chlorella Industry Co., Ltd., Fukuoka) was added twice daily (1.6 million cells/mL before yolk absorption, 800,000 cells/mL after yolk absorption). The larvae were reared for 80 days post-hatch, and specimens were collected at 0, 8, 16, 22, 31, 38, 45, 59, and 80 DAH, then anesthetized with MS-222 (NACALAI TESQUE, Inc., Japan) and fixed in 90 % ethanol.

Otolith Observation and Data Analysis

For yolksac larvae and preflexion larvae (with an incomplete notochord), the notochord length (NL,

measured from the tip of the upper jaw to the end of the notochord) was measured. For postflexion larvae and juveniles, standard length (SL, measured from the tip of the upper jaw to the base of the caudal fin, i.e., the end of the hypural bone) was measured. Measurements were taken with an ocular micrometer mounted on a stereomicroscope to the nearest 0.01 mm, and the resulting NL and SL values were recorded as body length (BL) for the respective larval stages. The larval developmental stages were categorized according to Okada et al. (Development of shishamo smelt larvae and juveniles under rearing conditions, Poster presented at: Annual Meeting of Japanese Society for Aquaculture Science; November 29, 2024; Okinawa, Japan).

Stage A: yolksac larval stage

Stage B: yolk absorbed but oil globule remains

Stage C: caudal fin rays appear

Stage D: notochord starts flexion and swim bladder visible

Stage E: dorsal fin rays appear

Stage F: post-flexion

Stage G: fin rays (excluding the pectoral fins) reach definitive count, black pigment cells appear in the fin membrane and head

Stage H: juvenile stage

Lapillus and sagitta otoliths were extracted under a stereomicroscope and embedded on a glass slide using nail resin (D Top Coat MA, Daiso Sangyo Co., Ltd., Hiroshima). Prior to observation, embedded otoliths were polished with 3 μ m grit lapping film (3 μ m lapping film, MARUTO instrument Co., Ltd., Tokyo) until the core was exposed. Observations were conducted under a biological microscope at 400–1000x magnification. Measurements of otolith radius and counts of increment rings were performed with images projected to a computer from a CCD camera (WRAYCAM–NOA2000, WRAYMER, Osaka) mounted on the microscope, using otolith increment measurement software (Ratoc System Engineering Co., Ltd., Tokyo).

Since otoliths of this species grow concentrically until the juvenile stage, their orientation relative to the body axis remains indistinguishable (rostrum or post-rostrum). Therefore, the otolith radius (OR) was measured as the maximum distance from the nucleus center to the edge.

Regression lines obtained from the relationship between the number of days post-hatch (x) and the number of increment rings formed outside each characteristic increment (y) were compared to $y = x$ using a t-test.

Field Collection of Larvae and Otolith Analysis

Field Collection

Wild Shishamo smelt larvae and juveniles were collected in the coastal waters in 5 to 10 m in front of the Mukawa and Sarugawa river mouths on June 20 and July 5, 2023, and on June 20–21 and July 8–9, 2024, using a sledge net (width: 1.5 m, height: 0.3 m, length: 5.0 m, mesh: 3.0 mm) (Fig. 1). Specimens were fixed in 90 % ethanol and brought back to the laboratory. Since the external morphology of Shishamo smelt larvae and juveniles closely resembles that of sympatric Pacific rainbow smelt *Osmerus dentex*, making identification by morphology alone difficult, the number of anal fin rays and the presence of lingual teeth were observed under a stereomicroscope for accurate identification (Yanagawa 1974). For the collected specimens, measurements were taken on video images captured by a video camera attached to a research-grade stereomicroscope (Nikon SMZ25, Nikon Corporation, Tokyo), using the image analysis system NIS-Elements D (Nikon Corporation, Tokyo). BL was measured as NL or SL, depending on developmental stage, consistent with the approach used for reared larvae.

Otolith Increment Analysis

Otolith embedding and increment ring observations were conducted following the same procedures as

those used for specimens from the rearing experiment.

The relationship between OR and BL was determined using the allometric equation fitted by the least-squares method with functions implemented in R version 4.5.1 (2025–06–13). To reconstruct individual growth histories, the Biological Intercept Method (Campana 1990) was used. Specifically, the allometric coefficients a and b were estimated for each individual by solving the following system of equations:

$$BL_0 = aOR_0^b$$

$$BL_{capture} = aOR_{capture}^b$$

where BL_0 and OR_0 represent the body length and otolith radius at hatching, respectively, and $BL_{capture}$ and $OR_{capture}$ represent those at the time of collection. Using the estimated coefficients (a and b), the body length at age i days (BL_i) was back-calculated from the corresponding otolith radius.

Results

Rearing Experiment

The results of examining body size and developmental stage by age in days showed that the mean body length \pm SD of larvae at hatching was 8.4 ± 0.29 mm (developmental stage A), 10.5 ± 0.60 mm at 8 DAH (Stage B), 11.1 ± 0.68 mm at 16 DAH (Stage B, C), 13.5 ± 1.12 mm at 22 DAH (Stage C, D), 14.6 ± 0.90 mm at 31 DAH (Stage D, E), 13.00 ± 0.66 mm at 38 DAH (Stage E), 14.9 ± 0.92 mm at 45 DAH (Stage E, F), 18.0 ± 0.93 mm at 59 DAH (Stage F, G), and 28.5 ± 4.63 mm at 80 DAH (Stage H) (Table 1, Fig. 2).

Both the sagitta and the lapillus otoliths were circular and grew concentrically until 45 DAH. After that, the lapillus otolith remained circular, but the sagitta developed into a teardrop shape as it grew. On both otoliths, a 1st check and 2nd check were observed (Fig. 3). The mean increment radius \pm SD of the 1st check was 12.2 ± 1.07 μ m (sagitta) and 12.4 ± 0.75 μ m (lapillus), which was not significantly different from the otolith radius at hatching, 12.7 ± 0.72 μ m (sagitta)

Table 1. Age (days), body length (BL; mm), otolith radius (OR; μm) of lapillus and sagitta, and developmental stage of reared larvae.

Age (days)	BL (mm)	OR (lapillus, μm)	OR (sagitta, μm)	Stage
0 DAH	8.4 ± 0.29	12.4 ± 0.69	12.7 ± 0.72	A
8 DAH	10.5 ± 0.60	13.6 ± 0.75	14.8 ± 1.33	B
16 DAH	11.1 ± 0.68	15.9 ± 1.97	18.4 ± 1.50	B, C
22 DAH	13.5 ± 1.12	15.5 ± 1.19	22.9 ± 2.48	C, D
31 DAH	14.6 ± 0.90	18.1 ± 1.68	35.4 ± 1.34	D, E
38 DAH	13.0 ± 0.66	20.8 ± 2.48	41.8 ± 5.66	E
45 DAH	14.9 ± 0.92	25.5 ± 2.85	73.0 ± 13.7	E, F
59 DAH	18.0 ± 0.93	44.3 ± 6.51	140.1 ± 23.1	F, G
80 DAH	28.5 ± 4.63	145.7 ± 19.3	398.2 ± 56.7	H

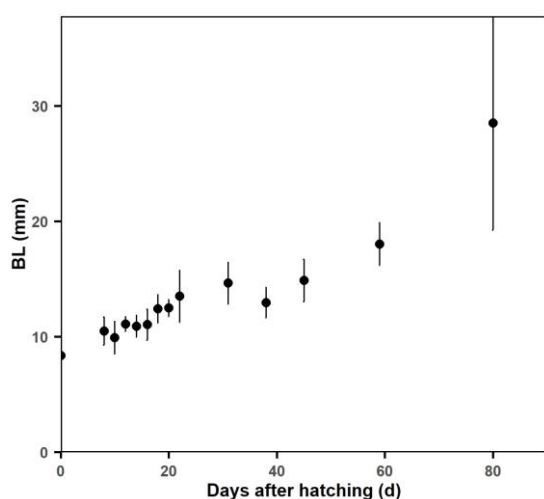


Fig. 2. Relationship between days after hatching and body length. Circles and vertical bars indicate mean values and standard deviations, respectively.

and $12.4 \pm 0.69 \mu\text{m}$ (lapillus) (t-test, $p = 0.09$, $p = 0.95$). The mean increment radius \pm SD of the 2nd check was $20.4 \pm 1.60 \mu\text{m}$ (sagitta) and $15.6 \pm 1.30 \mu\text{m}$ (lapillus). The relationship between DAH and OR (mean \pm SD, μm) is shown in Fig. 4. The mean otolith radius \pm SD for sagittae and lapilli respectively was $23.0 \pm 2.67 \mu\text{m}$ and $15.5 \pm 1.19 \mu\text{m}$ at 22 DAH, and $67.0 \pm 10.8 \mu\text{m}$ and $25.4 \pm 2.73 \mu\text{m}$ at 45 DAH.

The relationship between the number of increments after the 1st check on both otoliths (I_s , I_l) and age in days (A_c , days) was expressed by the following equations (Fig. 5):

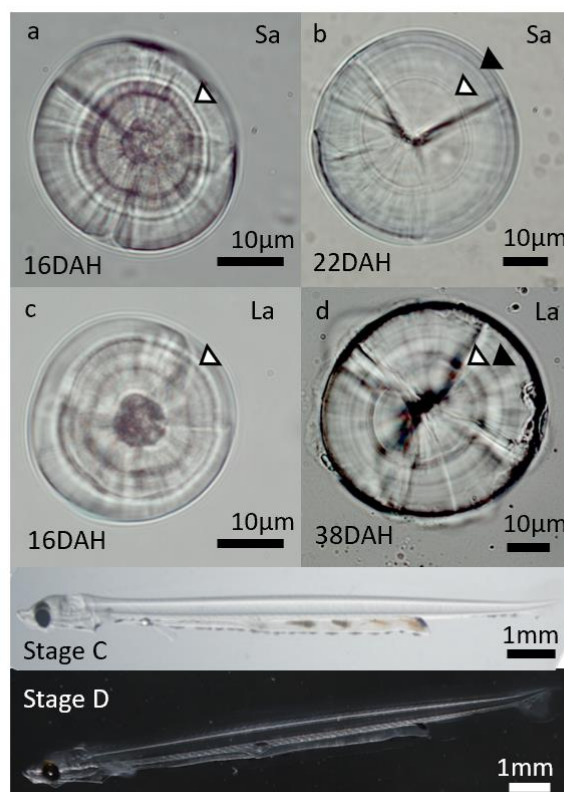


Fig. 3. Microphotographs of otoliths from *Spirinchus lanceolatus* larvae. a: sagitta from a 16-day-old larva, b: sagitta from a 22-day-old larva, c: lapillus from a 16-day-old larva, d: lapillus from a 38-day-old larva. The positions of the lower left tips of the open and solid triangles indicate 1st and 2nd checks, respectively. The larval images correspond to developmental stages C (top) and D (bottom), with a and c representing stage C, and b and d representing stage D.

Sagitta

$$I_s = 0.86A_c \quad (n = 38, r^2 = 0.992, p < 0.01)$$

Lapillus

$$I_l = 0.49A_c \quad (n = 24, r^2 = 0.932, p < 0.01)$$

The slope of the regression line was significantly different from 1 (t-test, both $p < 0.01$). The relationship between the number of increments after the 2nd check (I'_s , I'_l) and age in days (A_c , days) was expressed by the following equations (Fig. 5):

Sagitta

$$I'_s = 0.99A_c - 19.5 \quad (n = 26, r^2 = 0.996, p < 0.01)$$

Lapillus

$$I'_l = 0.61A_c - 16.3 \quad (n = 15, r^2 = 0.928, p < 0.01)$$

For the sagitta, the slope of the regression line was not significantly different from 1 (t-test, $p = 0.38$),



Fig. 4. Relationship between days after hatching and otolith radius. Circles and triangles indicate the mean values of lapillus and sagitta, respectively. Vertical bars represent the standard deviations.

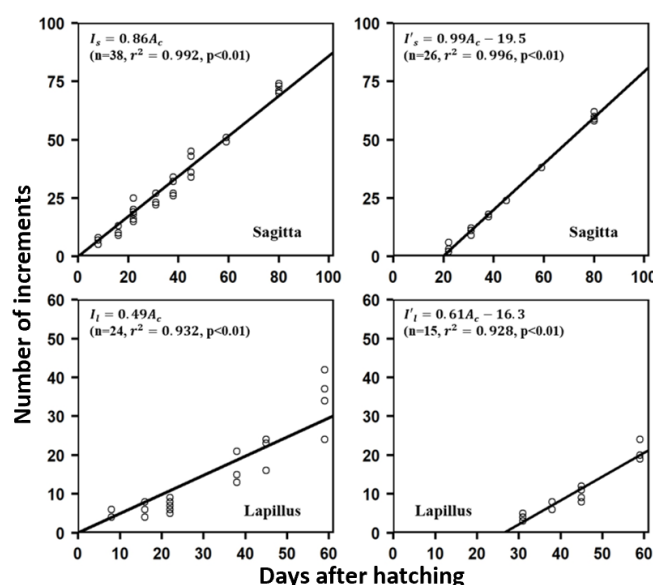


Fig. 5. Relationship between days after hatching and number of increments formed after 1st check (left) and 2nd check (right). Solid lines indicate regression lines fitted to each otolith type.

while for the lapillus, it was significantly different (t-test, $p < 0.01$). From the value of the intercept of the sagitta regression line, it was determined that the 2nd check is formed about 20 DAH.

Table 2. Wild-caught individuals for otolith analysis in 2023 and 2024: total individuals, number of larvae and juveniles, BL ranges.

		Year	
		2023	2024
BL range (mm)	Larvae	21.5-28.2	20.9-28.4
Number of sampels		35	50
BL range (mm)	Juvenile	28.6-33.0	28.5-41.3
Number of sampels		23	65
Total		58	115

Composition of Hatching Dates and Growth History of Wild-Caught larvae and Juveniles

The range of body lengths collected in 2023 was 20.1–33.1 mm (mean \pm SD: 25.6 ± 3.44 mm, $n = 134$), and in 2024 it was 20.9–41.3 mm (mean \pm SD: 29.9 ± 5.78 mm, $n = 123$). Of the 257 individuals, 173 were randomly selected (58 individuals in 2023, 115 in 2024) and used for otolith analysis (Table 2, Fig. 6). Based on the results of the rearing experiment, individuals with a BL 28.5 mm or greater were defined as juveniles.

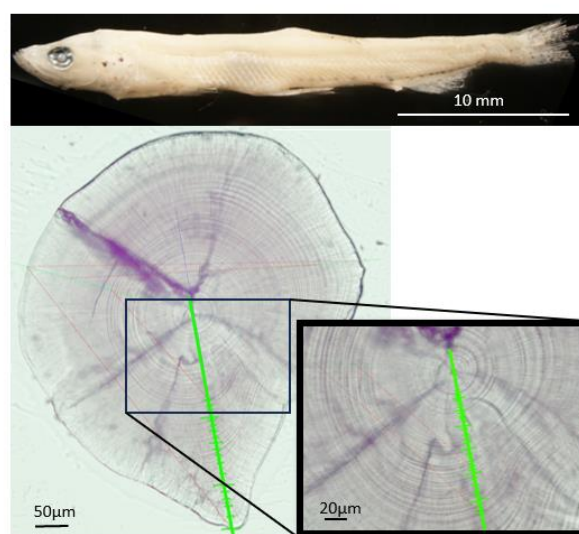


Fig. 6. Images of a wild-caught juvenile (fixed in ethanol) and corresponding otolith. Lines on the otoliths indicate increment counts.

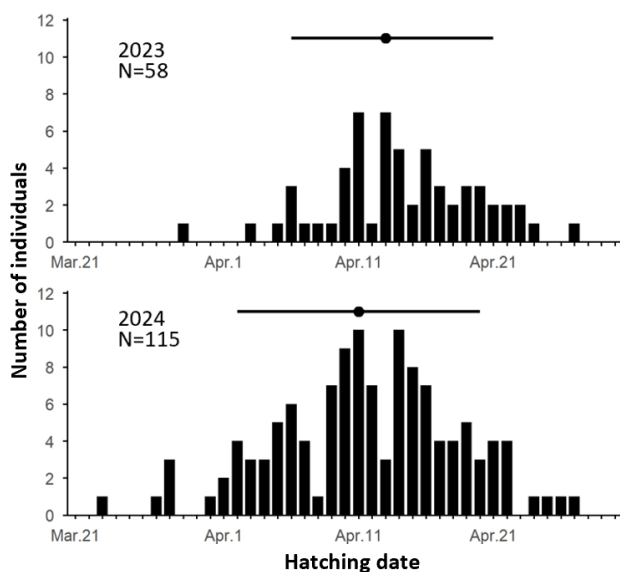


Fig. 7. Distributions of hatching dates in *Spirinchus lanceolatus* collected from the wild in 2023 (upper) and 2024 (lower). The circles and the bars indicate the median values and the ranges of 10th to 90th percentile.

In the rearing experiment, since the daily periodicity of otolith increment formation was confirmed for the sagitta after the 2nd check, the sagitta was used for age estimation in wild-caught individuals. In wild-caught individuals, the 2nd check was also observed on the sagitta, as in the reared individuals. The mean increment radius \pm SD was $20.2 \pm 0.76 \mu\text{m}$, which was not significantly different from the mean increment radius of the 2nd check in reared individuals ($20.4 \pm 1.60 \mu\text{m}$; t-test, $p = 0.26$).

Since the results of the rearing experiment showed that the 2nd check formed at 20 days after hatching, the age was estimated by adding 20 days to the number of increments after the 2nd check. In wild-caught individuals, increments after the 2nd check were clearly distinguishable in all specimens, supporting the reliability of age estimation. The range of ages for individuals collected in 2023 was 57–98 days, and for 2024 was 54–107 days. The composition of hatching dates, calculated from age and collection date, is shown in Fig. 7. The hatching date range was March 29 to April 27 in 2023 and March 23 to April 27 in 2024; the median hatching dates were April 14 in 2023 and April 12 in 2024. The length of the hatching period

based on the 10th–90th percentiles was 18 days (April 6 to April 23) in 2023 and 19 days (April 4 to April 21) in 2024.

The mean increment width after the 2nd check was 2.0–15.2 μm for the 2023 sample (2.3 μm at 30 days, 4.4 μm at 50 days, 8.5 μm at 70 days), and 2.0–16.5 μm for the 2024 sample (2.7 μm at 30 days, 5.0 μm at 50 days, 11.2 μm at 70 days); a pronounced tendency for increment width to rapidly increase after the 50th increment from the 2nd check was observed (Fig. 8a, b).

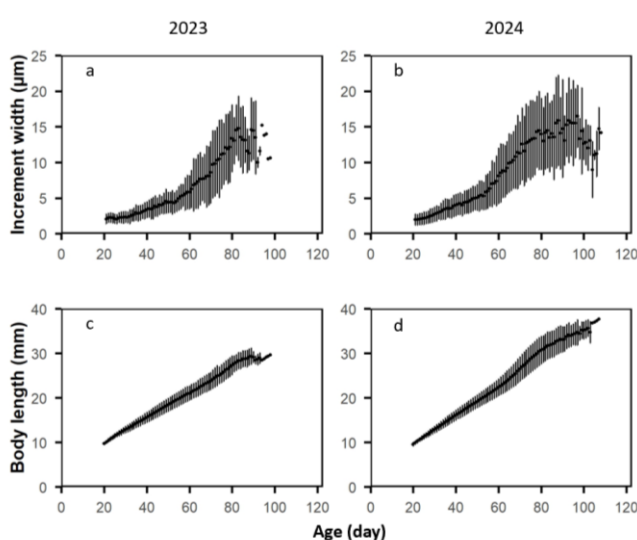


Fig. 8. Changes in daily increment width in the sagitta (upper) and back-calculated body lengths (lower) of *Spirinchus lanceolatus* in 2023 (a, c) and 2024 (b, d). Circles and vertical bars represent mean values and standard deviations, respectively.

The relationship between the radius of the sagitta otolith (OR) and body length (BL) in reared larvae and wild-caught larvae and juveniles showed a significant agreement with an allometric equation ($n = 249$, $r^2 = 0.959$, $p < 0.001$, Fig. 9). Therefore, this allometric relationship was adopted for body length back-calculation using the Biological Intercept Method. Although the Biological Intercept Method typically uses the body length at hatching (BL_0) and otolith radius at hatching (OR_0) obtained from rearing experiments (Campana 1990), this study instead used the body length (BL_{20}) and otolith radius (OR_{20}) at 20 DAH, when the 2nd check is formed. Based on the

rearing experiment, the mean \pm SD of body length at 20 DAH was 11.5 ± 0.62 mm, and the mean \pm SD of otolith radius was 19.6 ± 1.35 μ m; these values were used as BL_{20} and OR_{20} for back-calculation of each individual body length (Fig. 8c, d). As a result, the mean back-calculated body lengths \pm SD for 2023 and 2024 respectively were as follows: at 20 DAH, 11.4 ± 0.30 mm and 11.3 ± 0.36 mm; at 40 DAH, 17.0 ± 1.02 mm and 17.6 ± 1.13 mm; at 60 DAH, 21.8 ± 1.44 mm and 23.3 ± 1.95 mm; at 80 DAH, 27.6 ± 2.04 mm and 31.2 ± 3.01 mm (Fig. 8c, d).

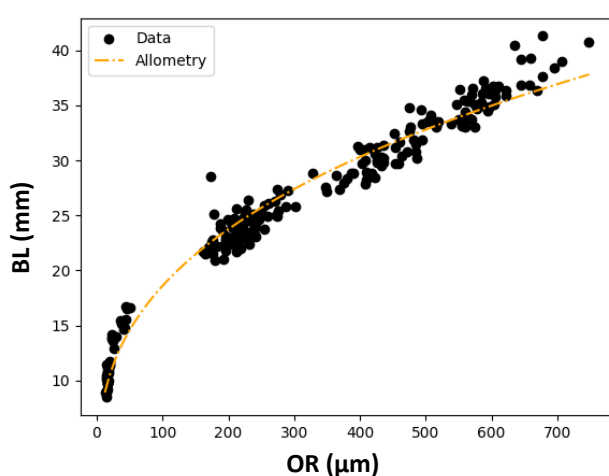


Fig. 9. Relationship between OR and BL in reared and wild-caught individuals. The dashed line represents the allometric regression curve.

Discussion

Validation of Daily Increment Formation

In many fish species, a check has been reported to form either during the transition from endogenous nutrition through yolk absorption to exogenous feeding or at the time of hatching (Brothers et al. 1976; Hayashi et al. 1989; Joh et al. 2005; Joh et al. 2008). In the present study, the 1st check on both the sagittal and lapillar otoliths of Shishamo smelt was also found to form at hatching. The radius of the hatching check is proportional to the diameter of the egg before hatching and may serve as an indicator of the nutritional and physiological condition status of female parental fish (maternal effect; Kajiwara et al. 2022). Thus, the 1st check in this species may likewise

provide important insights for understanding early survival processes.

The increments observed outside the 1st check on both the sagittal and lapillar otoliths did not show evidence of being formed at a rate of one increment per day. Furthermore, although the increments outside the 2nd check could not be demonstrated to form daily on the lapillar otoliths, they were confirmed to form one per day on the sagittal otoliths, and thus were considered appropriate to use daily increments.

It is known that fish growth is determined by the interaction between water temperature and feeding conditions (e.g., Takahashi et al. 2009). In this study, the feeding conditions were likely different from those experienced in the wild. However, the rearing experiment was conducted under water temperatures that simulated the natural environment (8.2 ± 0.83 °C, mean during 0–20 DAH), and no significant difference was observed in the radius of the 2nd check was also similar between reared and wild individuals. The trend in increment width formed after the 2nd check was also similar between the two groups. Therefore, using the number of days required for 2nd check formation under the rearing conditions (20 days) as a reference for estimating the age of wild-caught individuals is considered appropriate. To achieve more accurate estimations, it will be necessary to examine the effects of water temperature and feeding conditions on growth, the timing of check formation, and the radius of the checks in the future.

The reason daily increment formation could not be confirmed between the 1st check (12.2 ± 1.07 μ m, mean \pm SD) and 2nd check (20.4 ± 1.60 μ m, mean \pm SD) of the sagittal otoliths was likely because the increment width during this period is extremely narrow. The calculated mean increment width by dividing the mean difference in increment radius between the 1st and 2nd checks by the 20-day period required for 2nd check formation was about 0.41 μ m/day, making accurate counting by optical microscope observation difficult (Campana et al.

1987). In the case of the lapillus, growth was slower and the increment width even narrower compared to the sagitta, which likely accounts for the inability to confirm daily increment formation (Fig. 4). Similar phenomena have been reported in cold-water fish species such as the Atlantic herring *Clupea harengus* and European sardine *Sardina pilchardus* (Campana et al. 1987; Soares et al. 2021). Therefore, in the age estimation of cold-water fish species, which commonly feature increments that are difficult to discern for some period after hatching, it is rational to count only the increments that can be clearly distinguished from a certain point onward, and for the earlier period, supplement the estimation with check position and growth indicators.

The formation of the 2nd check did not occur at stage B when yolk absorption had been completed, but rather during the morphological shift to stage D, marked by the formation of the swim bladder (Table 1, Fig. 2). In species such as Pacific herring *Clupea pallasii* and Japanese amberjack *Seriola quinqueradiata*, it has been reported that the development of internal organs occurs in tandem with the swim bladder formation (Umeda and Ochiai 1973; Yamamoto 2001; Sakiyama 2006). Compared to species such as Japanese amberjack *Seriola quinqueradiata* and Striped jack *Caranx delicatissimus*, which have a rapid larval stage (Murai et al. 1987; Sakiyama 2006), the external morphology of Shishamo smelt tends to change more gradually (Table 1, Fig. 2). Therefore, the development of internal organs associated with the swim bladder formation can be considered a major structural change for Shishamo smelt. The formation of a check has been reported to occur in conjunction with significant structural changes, such as morphological transformations (Victor 1982; Penny and Evans 1985; Joh et al. 2005). Based on the above, it is likely that the formation of the 2nd check in this species would correspond to substantial internal morphological

changes triggered by the formation of the swim bladder.

In the sagitta, after the 2nd check, otolith increments became clearly distinguishable, which suggests a notable increase in the growth rate. In other fish species such as Japanese amberjack *Seriola quinqueradiata*, Chub mackerel *Scomber japonicus*, and Pacific herring *Clupea pallasii*, it has been reported that improvements in swimming ability during development are associated with accelerated growth (Yamamoto 2001; Murata et al. 2005; Sakiyama 2006). In this species as well, Stage D is a developmental stage characterized not only by the formation of the swim bladder but also by the formation of dorsal and anal fin primordia. This is accompanied by increased swimming ability, which, along with enhanced feeding capacity and the ability to move vertically in the water column, leads to increased feeding opportunities and thus promoted growth. On the other hand, the reason why the otolith increments could not be clearly distinguished in the lapillus even after the 2nd check may be that the growth of the otolith radius is slower in the lapillus than in the sagitta (Fig. 4), resulting in increment widths that were too narrow to be accurately counted under an optical microscope during this period (Campana et al. 1987).

Growth of Wild Larvae

Analysis of daily increments on the sagitta of wild-caught larvae estimated that the hatching period of the individuals surviving until June and July was from late March to late April in both years, assuming a 20-day period from hatching to the formation of the second check. The median hatching date was mid-April in both years, which closely matches the results of the annual downstream-migrating larval surveys conducted every April by the Hokkaido Aquaculture Promotion Corporation (Yoshida et al. 2021). This correspondence supports the reliability of hatching date estimation by otolith daily increment analysis and

indicates that age estimation is valid even for wild individuals.

Based on the validated age estimates obtained from otolith daily increment analysis, this study further clarified the growth trajectory of larvae hatched in April. Previous research identified relatively small larval body size on 1 July (24–27 mm) as one of the characteristics associated with years of poor recruitment (Yoshida et al. 2022). Considering the median hatch dates of the 2023 and 2024 cohorts, 1 July corresponds to 77 and 79 DAH, respectively. Using the growth model developed in this study, the back-calculated body lengths at that date were 26.3 mm for the 2023 cohort and 30.4 mm for the 2024 cohort (Fig. 8c, 8d). Both the 2023 and 2024 cohorts exhibited low stock abundance (Saibai suisan shikenjyou 2024, Saibai suisan shikenjyou 2025). Although there have been years in which larvae smaller than 27 mm did not lead to poor recruitment, no previous cases have been reported in which larvae exceeding 30 mm were associated with low stock abundance (Yoshida et al. 2022). Thus, the 2024 cohort—characterized by unusually large larvae despite low recruitment—represents a previously unobserved and potentially novel pattern in the early life history of this species.

In this study, through rearing experiments, daily increment formation was confirmed on the sagitta from the 2nd check to 80 days of age. In wild-caught individuals, some were older than 80 days of age; however, all of them continued to exhibit clearly distinguishable and regular otolith increments beyond this age. The oldest wild-caught individual examined was 107 days of age, indicating that daily increment formation persists at least up to this age. On the other hand, in older individuals, the sagitta changed shape from concentric circles to a droplet shape, making it unclear how long daily increment formation continues. Further rearing experiments are needed to determine how these changes in otolith morphology affect daily increment formation.

Acknowledgments

The authors thank Dr. H. Kudo of the Faculty of Fisheries Sciences, Hokkaido University for valuable comments on the manuscript. We extend our heartfelt gratitude to Mr. Kodai Takahashi and everyone at the Mariculture Fisheries Research Institute, Hokkaido Research Organization, for their substantial support in the rearing experiments, as well as for their exceptional assistance and consideration throughout the experimental period.

Furthermore, for their invaluable cooperation in larval sampling, we would like to thank Mr. Makoto Fujii of the Hokkaido Aquaculture Promotion Corporation and all involved, as well as the members of the Mukawa Fisheries Cooperative Association. I sincerely appreciate your support.

We are also grateful to Mr. Ryotaro Matsumoto, Mr. Kuuta Suzuki, and Mr. Kenta Wakabayashi, fellow members of the Laboratory of marine bioresource ecology at the Graduate School of Fisheries Sciences, Hokkaido University, for their cooperation in larval sampling. In addition, we extend our heartfelt thanks to all the students in the laboratory for their guidance in research methodology and for their ongoing advice and support in various aspects of my research.

Finally, we thank the three reviewers for their critical suggestions.

References

- Bailey, K. M., Canino, M. F., Napp, J. M., Spring, S. M., Brown, A. L. (1995). Contrasting years of prey levels, feeding conditions and mortality of larval walleye pollock *Theragra chalcogramma* in the western Gulf of Alaska. *Mar. Ecol. Prog. Ser.* 119: 11–23.
- Brothers, E. B., C. P. Mathews, R. Lasker (1976). Daily growth increments in otoliths from larval and adult fishes. *Fish. Bull.* 74: 1–8.
- Campana, S. E., Neilson, J. D. (1985). Microstructure of fish otoliths. *Can. J. Fish. Aquat. Sci.* 42: 1014–1032.
- Campana, S. E., Gagne, J. A., Munro, J. (1987). Otolith microstructure of larval herring (*Clupea harengus*): Image or reality? *Can. J. Fish. Aquat. Sci.* 44: 1922–1929.
- Campana, S.E. (1990). How reliable are growth back-

- calculations based on otoliths? *Can. J. Fish. Aquat. Sci.* 47: 2219–2227.
- Hayashi, A., Yamashita, Y., Kawaguchi, K., Ishii, T. (1989). Rearing method and daily otolith ring of Japanese sardine larvae. *Nippon Suisan Gakkaishi* 55: 997–1000.
- Hjort, J. (1914). Fluctuations in the great fisheries of northern Europe viewed in the light of biological research. *Rapp. P-v. Reun. Cons. int. Explor. Mer.* 20: 1–228.
- Hokkaido Aquaculture Promotion Corporation. (2017). *Yagai tyousa to shiiku jikken wo kumiawase ta shishamo no seitai kenkyuu [Shiiku gijyutsu kakuritsu ni mukete]*, Saibai gyogyo kousya sijyou daigaku. p. 3–7. <https://www.saibai.or.jp/wp-content/uploads/2018/10/sodateru479-1.pdf>. (accessed on 21 November 2025). (In Japanese).
- Ishida, R. (2016). Shigen kanri kaiyou kankyou shiriizu Shiiku jikken ni yoru shishamo no seitai kenkyuu. *Hokusuishidayori* 93: 10–15. (In Japanese).
- Ishida, R. (2020). Mukawa shishamo no sanran sojyou seitai. *Shiken kenkyuu ha ima* No.909. <https://www.hro.or.jp/upload/41405/ima909.pdf>. (accessed on 21 November 2025). (In Japanese).
- Jenkins, G. P. (1987). Age and growth of co-occurring larvae of two flounder species, *Rhombosolea tapirina* and *Ammotretis rostratus*. *Mar. Biol.* 95: 157–166.
- Joh, M., Takatsu, T., Nakaya, M., Higashitani, T., Takahashi, T. (2005). Otolith microstructure and daily increment validation of marbled sole *Pseudopleuronectes yokohamae*. *Mar. Biol.* 147: 59–69.
- Joh, M., Joh, T., Matsuura, T., Takatsu, T. (2008). Validation of otolith increment formation and the growth rate of fat greenling larvae. *Aquacult. Sci.* 56: 157–166.
- Kajiwarra, K., Nakaya, M., Suzuki, K., Kano, Y., Takatsu, T. (2022). Effect of egg size on the growth rate and survival of wild walleye pollock *Gadus chalcogrammus* larvae. *Fish. Oceanogr.* 31: 238–254.
- Laroche, J. L., Richardson, S. L., Rosenberg, L. L. (1971). Age and growth of a Pleuronectid, *Parophrys vetulus*, during the pelagic larval period in Oregon coastal waters. *Fish. Bull.* 80: 93–104.
- Maillet, G. L., Checkley, D. M. Jr. (1991). Storm-related variation in the growth rate of otoliths of larval Atlantic menhaden *Brevoortia tyrannus*: a time series analysis of biological and physical variables and implications for larval growth and mortality. *Mar. Ecol. Prog. Ser.* 79: 1–16.
- Mori, Y. (2003). Shishamo smelt. In: Y. Ueda, K. Maeda, H. Shimada, T. Takami (Eds.) *Fisheries and Aquatic Life in Hokkaido*. Hokkaido Shinbun Press, Hokkaido, p.86–89. (Japanese).
- Murai, M., Kato, K., Nakano, T., Takashima, F. (1987). Egg development and morphological changes of larval of striped jack *Caranx delicatissimus*. *Aquacult. Sci.* 34: 217–226. (In Japanese).
- Murata, O., Yamamoto, S., Ishibashi, R., Oka, Y., Yoneshima, H., Kato, K., Miyashita, S., Kumai, H. (2005). Egg development and growth of larval and juvenile cultured chub mackerel *Scomber japonicus* (Perciformes: Scombridae) in a captive spawning experiment. *Aquacult. Sci.* 53: 319–324. (Japanese).
- Nii, H., Murakami, K., Yoneda, T., Ueda, H. (2006). The relationship between spawning ground and physical river environmental conditions of shishamo smelt *Spirinchus lanceolatus*. *Nippon Suisan Gakkaishi* 72: 390–400. (In Japanese).
- Noichi, T., Matsuo, T., Senta, T. (1994). Hatching dates of the Japanese flounder settling at Yanagihama Beach in Nagasaki Prefecture, Japan. *Fish. Sci.* 60: 369–372.
- Omi, H. (1977). Shishamo no ran hassei to ran hassei sokudo ni oyobosu suion no eikyou. *Hokusuishigeppou* 35: 10–20.
- Penny, R. W., Evans, G. T. (1985). Growth histories of larval redbfish (*Sebastes* spp.) on an offshore Atlantic fishing bank determined by otolith increment analysis. *Can. J. Aquat. Fish. Sci.* 42: 1452–1464.
- Saibai suisan shikenjyou (2024). Shishamo dounan taiheyoiu kaiiki. 2024 nendo hokkaidou syuuhai kaiiki ni okeru syuyou gyosyu no shigen hyoukasyo, Dousouken suisan kenkyuu honbu, p. 297–311.
- Saibai suisan shikenjyou (2025). Shishamo dounan taiheyoiu kaiiki. 2025 nendo hokkaidou syuuhai kaiiki ni okeru syuyou gyosyu no shigen hyoukasyo, Dousouken suisan kenkyuu honbu, p. 316–333.
- Sakiyama, K. (2006). II-4 Seityou to seizan. Saibai gyogyo gijyutsu shiriizu No.12 Buri no syubyou seisan gijyutsu kaihatsu, Dokuritsu gyousei houjin suisan sougou kenkyuu sentaa, Kanagawa, p. 32–38.
- Soares, C., Ferreira, S., Ré, P., Teodósio, M., Santos, A. M., Batista, H., Baylina, N., Garrido, S. (2021). Effect of temperature on the daily increment deposition in the otoliths of European sardine *Sardina pilchardus* (Walbaum, 1792) larvae. *Oceans* 2: 723–737.
- Takahashi, M., Nishida, H., Yatsu, A., Watanabe, Y. (2008). Year-class strength and growth rates after metamorphosis of Japanese sardine (*Sardinops melanostictus*) in the western North Pacific Ocean during 1996–2003. *Can. J. Fish. Aquat. Sci.* 65: 1425–1434.
- Takahashi, M., Watanabe, Y., Yatsu, A., Nishida, H. (2009). Contrasting responses in larval and

- juvenile growth to a climate-ocean regime shift between anchovy and sardine. *Can. J. Fish. Aquat. Sci.* 66: 972–982.
- Torao, M., Kudou, S. (2013). Distribution and biochemical conditions of shishamo smelt *Spirinchus lanceolatus* larvae and juvenile in coastal waters off Mukawa River mouth. *Sci. Rep. Hokkaido Fish. Res. Inst.* 84: 31–38.
- Umeda, S., Ochiai, A. (1973). On the development of structure and function of the alimentary tract of the yellowtail from the larval to the juvenile stage. *Bull. Jpn. Soc. Sci. Fish.* 39: 923–930.
- Victor, B. C. (1982). Daily otolith increments and recruitment in two coral-reef wrasses, *Thalassoma bifasciatum* and *Halichoeres bivittatus*. *Mar. Biol.* 71: 203–208.
- Xie, S., Watanabe, Y., Saruwatari, T., Masuda, R., Yamashita, Y., Sassa, C., Konishi, Y. (2005). Growth and morphological development of sagittal otoliths of larval and early juvenile *Trachurus japonicus*. *J. Fish Biol.* 66: 1704–1719.
- Xie, S., Watanabe, Y. (2005). Hatch date-dependent differences in early growth and development recorded in the otolith microstructure of *Trachurus japonicus*. *J. Fish Biol.* 66: 1720–1734.
- Yamamoto, Y. (2001). VII. Shichigyo no hatsuiku, VIII. Syubyou seisan. Saibai gyogyo gijyutsu shiriizu No.7 Nishin no syubyou seisan gijyutsu, Syadan houjin Nihon saibai gyogyo kyokai, Tokyo, p. 31–50.
- Yanagawa, H. (1974). New discriminative characters between juveniles of two osmerid fishes, *Spirinchus lanceolatus* and *Osmerus eperlanus mordax*. *Bull. Fac. Fish. Hokkaido Univ.* 25: 163–168.
- Yoshida, H., Nii, H., Fujii M., Konno, Y., Kudou, S. (2021). Poor catch factors of shishamo smelt *Spirinchus lanceolatus* in the Pacific coast of southern Hokkaido (Note). *Sci. Rep. Hokkaido Fish. Res. Inst.* 99: 25–30. (In Japanese).
- Yoshida, H., Aataka, J., Fujii, M., Konno, Y., Nii, H. (2022). Declining body size of the Shishamo smelt *Spirinchus lanceolatus* on the Pacific coast of southern Hokkaido (Note). *Sci. Rep. Hokkaido Fish. Res. Inst.* 101: 31–38. (In Japanese).

Received: 16 December 2025 | Accepted: 13 February 2026 | Published: 22 February 2026